LETTER

doi:10.1038/nature10587

Electrically driven directional motion of a four-wheeled molecule on a metal surface

Tibor Kudernac[1,2]†*, Nopporn Ruangsupapichat[2]*, Manfred Parschau[3], Beatriz Maciá[1], Nathalie Katsonis[1,2]†, Syuzanna R. Harutyunyan[1], Karl-Heinz Ernst[3,4] & Ben L. Feringa[1,2]

Propelling single molecules in a controlled manner along an unmodified surface remains extremely challenging because it requires molecules that can use light, chemical or electrical energy to modulate their interaction with the surface in a way that generates motion. Nature's motor proteins[1,2] have mastered the art of converting conformational changes into directed motion, and have inspired the design of artificial systems[3] such as DNA walkers[4,5] and light- and redox-driven molecular motors[6–11]. But although controlled movement of single molecules along a surface has been reported[12–16], the molecules in these examples act as passive elements that either diffuse along a preferential direction with equal probability for forward and backward movement or are dragged by an STM tip. Here we present a molecule with four functional units—our previously reported rotary motors[6,8,17]—that undergo continuous and defined conformational changes upon sequential electronic and vibrational excitation. Scanning tunnelling microscopy confirms that activation of the conformational changes of the rotors through inelastic electron tunnelling propels the molecule unidirectionally across a Cu(111) surface. The system can be adapted to follow either linear or random surface trajectories or to remain stationary, by tuning the chirality of the individual motor units. Our design provides a starting point for the exploration of more sophisticated molecular mechanical systems with directionally controlled motion.

Figure 1a shows the molecular system and the distinctive design features that allow it to move upon electronic excitation in a preferred and linear direction across a surface (see Supplementary Information for synthesis and characterization of the molecules). The molecule has four chiral units based on the unidirectional rotary motors (Fig. 1b) that have been studied in solution[6,8] and liquid crystalline phases[17]. As illustrated in Fig. 1c, the rotary motors undergo geometric changes as a result of sequential configurational and conformational switching induced by electronic and vibrational excitation, respectively.

After sublimation onto a Cu(111) surface, individual molecules were imaged with a scanning tunnelling microscope (STM) at 7 K (see Supplementary Fig. 1 for details of the measuring and manipulation procedure). Imaging conditions are sufficiently mild that no changes are induced upon continuous scanning (Supplementary Fig. 2), with single molecules appearing as three or four joined-together lobes (each lobe corresponds to a rotary motor unit). Excitation can vary the STM contrast of individual stereoisomers between three and four lobe structures, reflecting excitation-induced geometrical changes in the molecule that lead to different conformers; but the original molecular feature always reappears (see Supplementary Information and Supplementary Figs 3 and 4 for details).

If the four motors all rotate in the same direction, linear translational motion of the molecule across the surface should occur through a paddlewheel type movement (Fig. 1d and e). Of all the possible isomers, this requirement is only met by the *meso*-(*R*,*S*-*R*,*S*) isomer sketched in Fig. 1a. Figure 2a shows a STM image of one such molecule on a Cu(111) surface, at its starting position. The STM tip is then positioned above the centre of the molecule to apply a voltage pulse larger than 500 mV, to induce movement that is observed by re-scanning the area under mild STM imaging conditions. Ten excitation steps result in the molecule travelling 6 nm across the surface along the trajectory indicated in Fig. 2b to the final position shown in Fig. 2c (see also Supplementary Movie 1). Figure 2e shows a selection of STM images recorded between electrically induced movements. (For additional examples, see Supplementary Fig. 6a.) We note that although backward movement is never observed, the trajectory is not perfectly straight because achieving simultaneous excitation of all motor units during each step is not trivial. Nonetheless, the data in Fig. 2 clearly show that the action of the motor units within the *meso*-(*R*,*S*-*R*,*S*) isomer induces directional propulsion of the molecule along the surface (see also Supplementary Information for a statistical analysis of the linearity of the translation and Supplementary Fig. 5).

In solution, unidirectional rotation of the motor units involves helix inversions and double bond isomerizations (Fig. 1c). On Cu(111), we anticipate that the propulsion of the molecule should also be the direct consequence of a combination of these two processes. In this context, we note that the conformation of porphyrins[18,19] and biphenyl molecules adsorbed on surfaces[20] has been switched through STM-induced vibrational excitation. Similarly, configurational switching (isomerization) of azobenzene[21] and 2-butene[22] on surfaces has been realized by exciting electronic transitions with tunnelling electrons in a manner analogous to excitation by a photon[23].

Our view of the configurational and conformational changes resulting in the movement of a single *meso-(R,S-R,S)* molecule along the surface is sketched in Fig. 1e. Electronic excitation induces double-bond isomerization that is followed by helix inversion (see Fig. 1c), resulting in paddlewheel-like motion pushing the entire molecule one step forward. Movement is of course possible only if the adsorption energy of the molecule is less than the energy released in the isomerization step upon excitation. Because the motor units are highly strained helical systems, their aromatic parts cannot align parallel to the surface (Fig. 1e) but are oriented edge-on and physisorbed through their hydrogen atoms. This leads to binding energies for individual motor units considerably below the 0.5 eV observed with, for example[24], parallel benzene on Cu(111). Finally, we note that one paddlewheel-like motion corresponds to 0.7 nm of forward movement and that ten excitation events should thus result in the molecule having traversed approximately 7 nm. In practice, we observe near-ideal linear movement resulting in 6 nm after ten steps (Fig. 2b).

In addition to changing their positions, molecules also exhibit a modified STM contrast after movement. Irreversible changes in the structure of the molecule, however, are excluded, as the contrast changes are fully reversible. To explore this effect further, the STM

[1]Centre for Systems Chemistry, Stratingh Institute for Chemistry, University of Groningen, Nijenborgh 4, 9747 AG Groningen, The Netherlands. [2]Zernike Institute for Advanced Materials, University of Groningen, Nijenborgh 4, 9747 AG Groningen, The Netherlands. [3]Nanoscale Materials Science, Empa, Swiss Federal Laboratories for Materials Science and Technology, Überlandstrasse 129, CH-8600 Dübendorf, Switzerland. [4]Department of Chemistry, University Zurich, Winterthurerstrasse 190, CH-8057 Zürich, Switzerland. †Present address: MESA+ Institute for Nanotechnology, University of Twente, PO Box 217, 7500 AE, Enschede, The Netherlands.
*These authors contributed equally to this work.

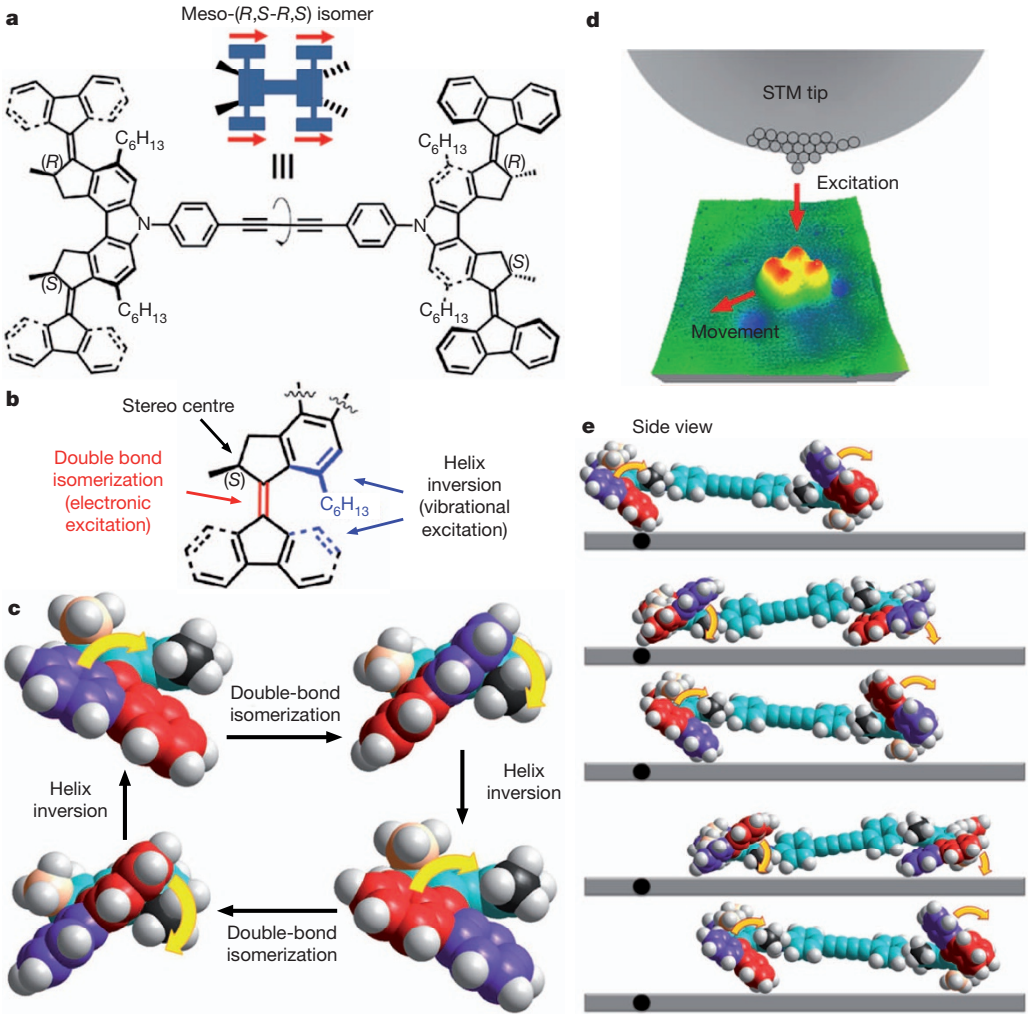

Figure 1 | Structure of the four-wheeled molecule. **a**, Structure and cartoon representation of the *meso*-(*R*,*S*-*R*,*S*) isomer. Red arrows indicate the direction in which the rotary action of the individual motor units propels the molecule. (*R*) and (*S*) indicate the absolute configurations at the stereogenic centres. The black solid and dashed wedges of the cartoon indicate the orientations of the methyl groups, respectively. **b**, Structural details of the rotary motor unit. The double bond (red) functions as the axle in rotation and undergoes *trans*-to-*cis* isomerization when electronically excited. Interconversion between helical conformers, arising from steric overcrowding in the region highlighted in blue, is achieved by vibrational excitation. The stereocentre in the cyclopentane ring determines the stability of each conformer and the direction of rotation of the motor. **c**, Schematic representation of the 360° rotation of the rotary motor, involving two double-bond isomerization steps and two helix inversion steps. Different colours in the model highlight the different positions of atoms during the rotor action. For clarity, the hexyl groups are substituted by methyl groups. **d**, Schematic representation of the experiment. The bias voltage U is applied to the sample. Electrons tunnelling through the molecule excite vibrational and electronic states and induce translational movement on the surface. **e**, Molecular model representation (side view) of the paddlewheel-like motion of the four-wheeled molecule (see also Supplementary Movie 4).

tip was positioned above one lobe of the molecule and voltage pulses of between 200 and 350 mV were applied to induce contrast modification without displacement (Fig. 3a and b; Supplementary Movie 2). The threshold for inducing conformational changes within the motor units, without movement, is 200 mV. This is illustrated by the action spectrum in Fig. 3c, which is related to the vibrational density of states[25], with the threshold bias of 200 mV corresponding to the excitation of the C=C double bond stretching vibration[26] (204 meV, ~1,600 cm^{-1}) that induces the helix inversion of the rotor unit.

Another insight into the mechanism of propulsion is provided by the polarity dependence of our experiments. Figure 3d shows that negative pulses of −1,500 mV induce contrast modifications but no movement. We note that vibrational excitation by inelastically tunnelling electrons is polarity independent. In contrast, a positive pulse of +1,500 mV, applied with the same tip on the same molecule and in the same position, induces a reproducible translation of the molecule (Fig. 3d). The polarity dependence of the movement points clearly to the electronic origin of the motor rotation. The corresponding action spectrum (Fig. 2d) of the molecule suggests the presence of the lowest unoccupied molecular orbital (LUMO) at around 500 meV above the Fermi level. Resonant tunnelling into the LUMO of the molecule will lead to transient excitation of the molecule by forming a negative ion resonance[27]. This results in excitation analogous to light-induced double-bond isomerization.

We excluded from our experiments all cases of dragging[14–16] or pick-up-and-drop[28] with the STM tip, and random or directional thermal diffusion[12,13] of molecules was not observed under the experimental conditions in any of the measurements. We also exclude vibrationally induced lateral hopping (activated diffusion) as a cause for the movement because the minimum energy of 500 mV needed to induce it is well above relevant vibrational energies[29]. Instead, the polarity dependence and the very low tunnelling currents during manipulation support an electronic excitation mechanism.

Additional experimental corroboration for electrically driven directional motion comes from two series of experiments probing the impact of the chirality and geometry of the molecule on its motion (Fig. 4). A key point is that improper orientation ('wrong landing') of the *meso*-isomer on the surface completely changes its behaviour

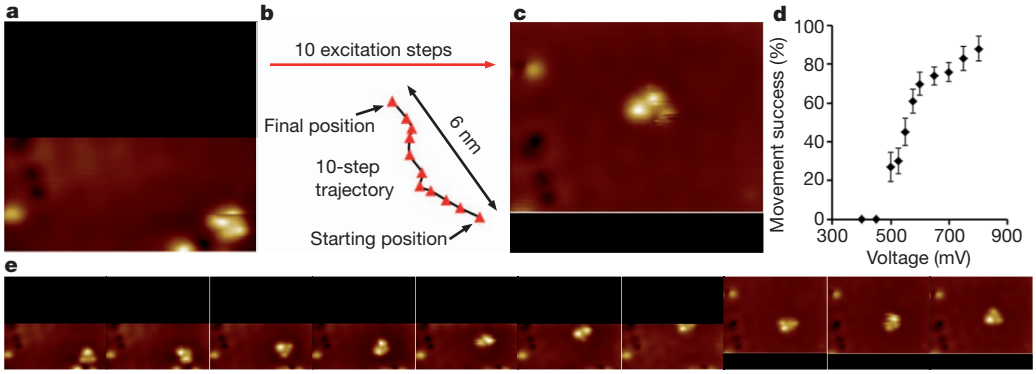

Figure 2 | Linear movement of the *meso*-(*R*,*S*-*R*,*S*) isomer. **a**, STM image (imaging parameters: area 10.2 nm × 9.3 nm, current $I = 74$ pA, $U = 47$ mV) of the initial position. The black area was scanned only after the molecule moved into it. **b**, Trajectory depicting the individual steps taken (see Supplementary Movie 1). **c**, Final position after ten consecutive voltage pulses. **d**, The action spectrum for movement shows a voltage threshold at 500 mV. Each data point represents 8 to 40 manipulations performed on various molecules ($I = 30$–50 pA). Error bars represent the standard deviation from the probability for successful events (see equation (1) in the Supplementary Information). **e**, STM frames corresponding to individual steps of the trajectory in **b** excluding starting and final position.

(Fig. 4a–c): the changes in contrast arising from helix inversions occur (Supplementary Fig. 6b), but the molecule shows no translational movement upon manipulation. In the second series of experiments, individual (*R*,*R*-*R*,*R*) or (*S*,*S*-*S*,*S*) enantiomers of the racemate adsorbed on the surface were found to spin and randomly move across the surface as illustrated in Fig. 4d–f, which shows a molecule that travels an overall distance of only 3 nm after 40 excitation steps (see also Supplementary Figs 5 and 6c for STM image frames and

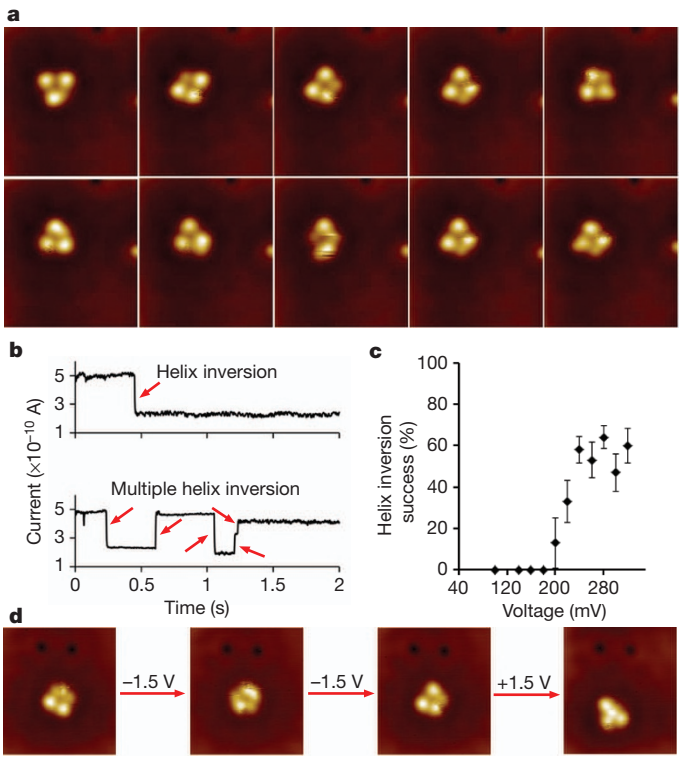

Figure 3 | Helix inversion at lower bias voltage and polarity dependence of propulsion. **a**, Voltage pulses between 200 and 350 mV lead to conformational changes but no movement (7.0 nm × 7.8 nm, $I = 43$ pA, $U = 47$ mV). **b**, Steps in the real-time traces (red arrows) of the tunnelling current ($U = 200$ mV) indicate the internal conformational changes of the molecule. **c**, The threshold voltage for helix inversion is 200 mV (>200 manipulations, $I = 30$–50 pA). Error bars represent the standard deviation from the probability for successful events (see equation (1) of the Supplementary Information). **d**, Negative bias (tunnelling from the sample to the tip) induces contrast changes but no movement (7.0 nm × 7.8 nm, $I = 43$ pA, $U = 47$ mV). Positive voltage pulses lead to movement and helix inversion.

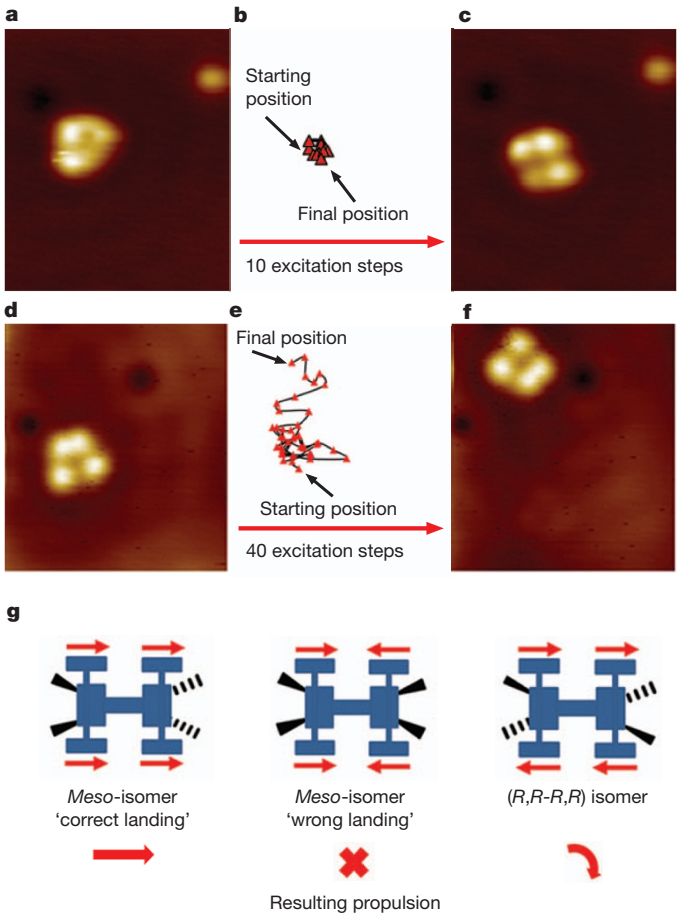

Figure 4 | Control over motion by the geometries of the four motors. **a**–**c**, Absence of motion of a 'wrongly landed' *meso*-isomer. **a**, STM image of a 'wrongly landed' *meso*-isomer (7.0 nm × 7.8 nm, $I = 74$ pA, $U = 47$ mV). **b**, Plot of all positions occupied by this *meso*-isomer after each manipulation (see Supplementary Fig. 6b for individual STM images). **c**, STM image of the molecule after ten voltage pulses. **d**–**f**, Random motion of a single (*R*,*R*-*R*,*R*) or (*S*,*S*-*S*,*S*) enantiomer. **d**, STM image at initial position (7.0 nm × 7.8 nm, $I = 47$ pA, $U = 47$ mV). **e**, Trajectory of 40 individual steps (see Supplementary Movie 3 and Supplementary Fig. 6c for individual STM images). **f**, STM image at final position. **g**, Sketch of directionality of movement induced by concerted rotation of the motor units. Two distinct 'landing geometries' of the *meso*-isomer lead to either directional movement or to no movement at all. (*R*,*R*-*R*,*R*) or (*S*,*S*-*S*,*S*) isomers move randomly.

Supplementary Movie 3). We note also that in contrast to the 'correctly landed' *meso*-isomer (Fig. 2), the STM appearance is dominated by four lobes (Fig. 4; for details of the STM appearance see Supplementary Fig. 4).

As sketched in Fig. 4g, these differences in motion are readily explained by the chirality and geometry of the molecule on the surface. In the case of the *meso*-isomer, two geometries need to be considered because free rotation around the bisalkyne C–C single bond of the frame is locked upon physisorption (Figs 1a and 4g). When the *meso*-(*R*,*S*-*R*,*S*) isomer is adsorbed on the surface in the proper orientation ('correct landing'), the four motor units can act in concert so that conrotatory motion moves the molecule along. In contrast, in the 'wrongly landed' *meso*-(*R*,*S*-*R*,*S*) isomer the combined effects of the motor units cancel out and thus preclude translational movement (Fig. 4a–c and g). And in the (*R*,*R*-*R*,*R*) or (*S*,*S*-*S*,*S*)-enantiomers of the racemic mixture, the motor units on opposite sides of the molecule will rotate in a disrotatory fashion and, in an ideal case, cause these molecules to spin; in a non-ideal case, the molecules exhibit random translational motion in addition to the spinning motion (Fig. 4d–f and g).

The directional and exclusively forward movement of the 'correctly landed' *meso*-isomer, the lack of movement of the 'wrongly landed' *meso*-isomer and the random movement of individual molecules of the racemic isomer are direct consequences of the molecular design and provide compelling evidence that the translational movement originates from the concerted action of the molecular motor units (Fig. 4g). A single molecule with intrinsic motor functions is thus capable of converting an external energy input into unidirectional movement along a surface.

METHODS SUMMARY

STM manipulations were performed with a custom-built low-temperature STM under ultrahigh vacuum conditions with base pressure below 10^{-10} mbar at a temperature of 7 K. To ensure that no molecule manipulation occurs upon scanning, constant-current STM images were recorded with positive voltages below 60 mV and tunnelling currents between 30 and 100 pA. The Cu(111) surface was cleaned by 30 min of argon sputtering followed by 15 min of annealing at 820 K. Molecules were sublimed at 553 K for 2 min on the pre-cooled clean surface held at 40 K. For single-molecule manipulation (see Supplementary Information) the STM tip was positioned over the molecule and the feedback loop was then switched off. A voltage pulse between the steady STM tip and the surface was applied for a few seconds while recording the tunnelling current. A step-like variation in tunnelling current indicated a manipulation step and rescanning of the area revealed the type of manipulation. Determining the threshold voltages for the helix inversion and propulsion was performed with currents between 30 and 50 pA.

Received 10 January; accepted 15 September 2011.

1. Schliwa, M. & Woehlke, G. Molecular motors. *Nature* **422,** 759–765 (2003).
2. van den Heuvel, M. G. L. & Dekker, C. Motor proteins at work for nanotechnology. *Science* **317,** 333–336 (2007).
3. Ismagilov, R. F., Schwartz, A., Bowden, N. & Whitesides, G. M. Autonomous movement and self-assembly. *Angew. Chem. Int. Edn Engl.* **41,** 652–654 (2002).
4. Lund, K. *et al.* Molecular robots guided by prescriptive landscapes. *Nature* **465,** 206–210 (2010).
5. Gu, H., Chao, J., Xiao, S.-J. & Seeman, N. C. A proximity-based programmable DNA nanoscale assembly line. *Nature* **465,** 202–205 (2010).
6. Browne, W. R. & Feringa, B. L. Making molecular machines work. *Nature Nanotechnol.* **1,** 25–35 (2006).
7. Kay, E. R., Leigh, D. A. & Zerbetto, F. Synthetic molecular motors and mechanical machines. *Angew. Chem. Int. Edn Engl.* **46,** 72–191 (2007).
8. Koumura, N., Zijlstra, R. W. J., van Delden, R. A., Harada, N. & Feringa, B. L. Light-driven molecular rotor. *Nature* **401,** 152–155 (1999).
9. Balzani, V., Credi, A., Raymo, F. M. & Stoddart, J. F. Artificial molecular machines. *Angew. Chem. Int. Edn Engl.* **39,** 3348–3391 (2000).
10. van Delden, R. A. *et al.* Unidirectional molecular motor on a gold surface. *Nature* **437,** 1337–1340 (2005).
11. Green, J. E. *et al.* A 160-kilobit molecular electronic memory patterned at 1011 bits per square centimeter. *Nature* **445,** 414–417 (2007).
12. Shirai, Y., Osgood, A. J., Zhao, Y., Kelly, K. F. & Tour, J. M. Directional control in thermally driven single-molecule nanocars. *Nano Lett.* **5,** 2330–2334 (2005).
13. Wong, K. L. *et al.* A molecule carrier. *Science* **315,** 1391–1393 (2007).
14. Gimzewski, J. K. & Joachim, C. Nanoscale science of single molecules using local probes. *Science* **283,** 1683–1688 (1999).
15. Grill, L. *et al.* Rolling a single molecular wheel at the atomic scale. *Nature Nanotechnol.* **2,** 95–98 (2007).
16. Chiaravalloti, F. *et al.* A rack-and-pinion device at the molecular scale. *Nature Mater.* **6,** 30–33 (2007).
17. Eelkema, R. *et al.* Nanomotor rotates microscale objects. *Nature* **440,** 163 (2006).
18. Iancu, V., Deshpande, A. & Hla, S.-W. Manipulating Kondo temperature via single molecule switching. *Nano Lett.* **6,** 820–823 (2006).
19. Qiu, X. H., Nazin, G. V. & Ho, W. Mechanisms of reversible conformational transitions in a single molecule. *Phys. Rev. Lett.* **93,** 196806 (2004).
20. Lastapis, M. *et al.* Picometer-scale electronic control of molecular dynamics inside a single molecule. *Science* **308,** 1000–1003 (2005).
21. Alemani, M. *et al.* Adsorption and switching properties of azobenzene derivatives on different noble metal surfaces: Au(111), Cu(111), and Au(100). *J. Phys. Chem. C* **112,** 10509–10514 (2008).
22. Sainoo, Y., Kim, Y., Komeda, T., Kawai, M. & Shigekawa, H. Observation of *cis*-2-butene molecule on Pd(110) by cryogenic STM: site determination using tunneling-current-induced rotation. *Surf. Sci.* **536,** L403–L407 (2003).
23. Henzl, J. & Morgenstern, K. An electron induced two-dimensional switch made of azobenzene derivatives anchored in supramolecular assemblies. *Phys. Chem. Chem. Phys.* **12,** 6035–6044 (2010).
24. Lukas, S., Vollmer, S., Witte, G. & Wöll, C. Adsorption of acenes on flat and vicinal Cu(111) surfaces: step induced formation of lateral order. *J. Chem. Phys.* **114,** 10123–10130 (2001).
25. Ueba, H. & Persson, B. N. Action spectroscopy for single-molecule motion induced by vibrational excitation with a scanning tunneling microscope. *Phys. Rev. B* **75,** 041403 (2007).
26. Parschau, M., Passerone, D., Rieder, K.-H., Hug, H. J. & Ernst, K.-H. Switching the chirality of a single adsorbate. *Angew. Chem. Int. Edn Engl.* **48,** 4065–4068 (2009).
27. Seideman, T. Current-driven dynamics in molecular-scale devices. *J. Phys. Condens. Matter* **15,** R521, doi:10.1088/0953-8984/15/14/201 (2003).
28. Eigler, D. M., Lutz, C. P. & Rudge, W. E. An atomic switch realized with the scanning tunnelling microscope. *Nature* **352,** 600–603 (1991).
29. Parschau, M., Rieder, K.-H., Hug, H. J. & Ernst, K.-H. Single-molecule chemistry and analysis: mode-specific dehydrogenation of adsorbed propene by inelastic electron tunneling. *J. Am. Chem. Soc.* **133,** 5689–5691 (2011).

Supplementary Information is linked to the online version of the paper at www.nature.com/nature.

Acknowledgements This research was supported by the Netherlands Organization for Scientific Research (NWO-CW) (B.L.F. and T.K. through a VENI grant), the Swiss Secretary for Education and Research and the Swiss National Science Foundation (K.-H.E. and M.P.), and the European Research Council (ERC advanced grant 227897 to B.L.F.).

Author Contributions N.R., B.M., S.R.H. and B.L.F. designed the four-wheeled molecule and N.R. conducted its synthesis and characterization. T.K., M.P., N.K. and K.-H.E. designed the STM experiments and contributed to their interpretation. T.K. and M.P. performed the STM experiments at Empa. T.K., K.-H.E. and B.L.F. wrote the manuscript. S.R.H., K.-H.E. and B.L.F. conceived and guided the research. All authors discussed the results and implications and commented on the manuscript at all stages.

Author Information Reprints and permissions information is available at www.nature.com/reprints. The authors declare no competing financial interests. Readers are welcome to comment on the online version of this article at www.nature.com/nature. Correspondence and requests for materials should be addressed to S.R.H. (s.harutyunyan@rug.nl), K.H.E. (karl-heinz.ernst@empa.ch) or B.L.F. (b.l.feringa@rug.nl).